SEMARAK ILMU PUBLISHING

Journal of Advanced Research in Fluid Mechanics and Thermal Sciences

Journal homepage:
https://semarakilmu.com.my/journals/index.php/fluid_mechanics_thermal_sciences/index
ISSN: 2289-7879

Design and Characteristics of a New Pre-Evaporation Chamber Geometry for Low-Grade Palm Oil Fuel Evaporation for Micro Gas Turbine Application

Mohammed Raad Abdulwahab[1,2], Khaled Ali Mohammad Al-attab[1,*], Mohamad Yusof Idroas[1]

[1] School of Mechanical Engineering, Universiti Sains Malaysia, Engineering Campus, 14300, Nibong Tebal, Penang, Malaysia
[2] Northern Technical University, Technical College of Mosul, Mosul, Iraq

ARTICLE INFO

Article history:
Received 8 January 2022
Received in revised form 20 March 2022
Accepted 23 March 2022
Available online 28 April 2022

Keywords:
Pre-evaporation chamber; combustion; palm oil; MGT; evaporation rate

ABSTRACT

Recent increase in fuel prices, greenhouse emissions, global warming issue, as well as future predictions regarding fossil fuel depletion concerns have prompted widespread research on carbon-neutral renewable liquid biofuels as an alternative of petroleum fuels. In the present study, a numerical approach was used to design and optimize a novel design of pre-evaporation chamber, to pre-evaporate crude palm oil fuel using exhaust gas recycling to allow partially premixed fuel vapors to be introduced to the main combustion chamber. Discrete Phase Model (DPM) and species non-premixed model used in ANSYS-FLUENT software to simulate fuel evaporation. The pre-chamber optimization included the addition of variable number of revolve geometry to the walls to induce turbulence and to enhance the cyclonic motion caused by the tangential hot exhaust gas inlets with different fuel injection configurations. The number of revolves was varied in the range of 5-8 and diameter range of 40-90 mm with three injector configurations. The results revealed that the optimum chamber geometry consist of 7 revolves with 70 mm diameter with fuel evaporation rate about 0.0023kg/s and fuel evaporation percentage about 89%. Increasing the exhaust gas temperature from 950 °C up to 1050°C did not show a significant fuel evaporation enhancement. Results also showed that the evaporation enhancement is proportional to the number of fuel injectors where evaporation increased gradually from 73% to 89% when increasing number of injectors from 1 to 3.

1. Introduction

The rapid development in industry towards the full automation and the other aspects of modern human life are heavily dependent on fossil fuel consumption as it supplies more than 80% of the global energy requirements. Power generation in Malaysia mainly depends on three significant types of fossil fuel (coal, natural gas and fuel oil). Fossil fuels combustions leads to generate greenhouse gases to the surroundings [1]. Therefore, the energy requirement is rapidly increasing leading to serious concerns about finding alternatives for fossil fuels as their depletion is inevitable. However,

* *Corresponding author.*
E-mail address: khaled@usm.my

https://doi.org/10.37934/arfmts.94.2.184199

due to the increase of greenhouse emissions released from fossil fuel combustion, environmental issues have increased. One of the most important environmental issues is global warming due to increasing rate of greenhouse gases generation. For this reason, using alternative fuels instead of conventional fuel as well as efficient combustion technology become urgent [2-4]. Recently, renewable energy was presented as solution for global warming and shortage of fossil fuel issues. Malaysia has a huge resource of biomass currently utilized to generate electricity, such as waste of palm oil [5]. In the last few years, using renewable energy sources such as biomass, solar energy, wind energy, hydropower and geothermal has been developed. Furthermore, biogas from wastewater effluent, municipal solid wastes (MSW), animal waste and agricultural by-products have been used for combined heat and power (CHP) generation purposes [6-10]. However, liquid biofuels are of an utmost importance as they can directly replace petroleum products in transport, aviation and power sectors. The Butyl Nonanoate biofuel performance was experimentally tested then compared to Hydrogenated Renewable Jet (HRJ) fuel and JP-8. The phase doppler particle technique was used to examine atomization properties. The emissions of CO were lower when using Butyl Nonanoate as compared to JP-8, in contradict to HRJ biofuel which revealed Co increment as compared to JP-8 [11]. Similar results were observed when using blends of biofuels with jet-A1 with drop in CO and slight elevation in NOx emissions [12, 13]. Another technology to enhance the combustion of liquid biofuels is the medium or severe low oxygen dilution (MILD). An experimental study has been done on pre-vaporized liquid fuels burning in a reverse-flow MILD combustor under high pressures. The results revealed that the stability of combustion is dependent mainly on fuel type, with n-heptane being the most unstable due to its fast ignition under all high pressure conditions studied [14]. Another combustion technology getting more attention lately is the flameless combustion achieved through intensive internal heat circulation or highly preheated air supply. Experimental and numerical analysis of combustor with double stage combustor reaching flameless combustion with liquid fuels examined variable inputs of thermal heat in the range of 20-60 kW with heat intensity release of 5–15 MW/m^3. Characteristics of Combustion and unwanted emissions were studied for different three fuels, kerosene, diesel and gasoline. Computational fluid dynamics (CFD) analysis of the characteristics flow reveals that reducing the diameter of exit port of the primary chamber increases the recirculation rate of products and helped in reaching the mode of flameless combustion [15]. Swirl flow was also proposed to enhance heat circulation allowing to attain flameless combustion with heat liberate intensity of 5.4–21 MW/m^3 using kerosene fuel. CFD analysis showed enhancement in flameless combustion by increasing chamfer radius, recirculation of the combustion products and fuel residence time [16]. The effect of the high injection pressure and ambient condition of blended bio-diesel on spray features were numerically investigated using (CFD) analysis. The results revealed that more spray penetration length with fewer spray remarkably influence the formation of bio-diesel blends compared to pure diesel at high injection pressure and surrounding temperature [17].

Large portion of research on liquid biofuels is dedicated for gas turbine technology as a major beneficiary of such fuels. The palm methyl ester (PME) combustion features as a replacement fuel for gas turbines have been investigated experimentally with preheated air at 673 K. Results showed that combustion features of PME are same to those of diesel fuel. Besides, it gives an indication that NOx emissions can be lessen by using PME rather than diesel fuel for gas turbines [18]. Another experimental investigation on gas turbine fuels compared between two liquid fuels: biodiesel and mixture of biodiesel with pyrolysis by-product. These two fuels were compared with a kerosene as benchmark. In terms of stability and combustion, it is suggested that the saturated blend would be a workable candidate for gas turbine power generation [19]. Similarly, blends of kerosene with waste tyre pyrolysis oil (up to 50%) achieved stable turbine operation but with elevation in CO and NOx

emissions [20]. The combustion analysis of an extremely oxygenated and economically feasible viscous fuel such as glycerol in MGT has been conducted. Results revealed that such fuel provided environmental advantages in terms of the reduction in NOx emission and PM concentration [21]. Utilizing the well-established and low-cost turbocharger technology for the development of small-scale MGT is a promising alternative to reduce the cost of MGT. However, a small-scale combustion chamber has to be developed since turbocharges do not include it. Combustion chamber design for turbocharger-based two-stage MGT was performed using CFD simulation. Different chamber and flame tube geometries were used with species transport and non-premixed combustion models in order to find the optimize chamber design [22]. Fuel spray patterns and atomization quality with different sizes of injectors and fuel flow rates were experimentally investigated to study their effect on quality of combustion [23]. The original chamber design was not fully optimized for liquid fuels, thus, further CFD optimization utilized discrete phase model (DPM) to simulate fuel evaporation. The flame tube was extended with fuel pre-evaporation portion resulting of low CO emissions of 99 ppm and NOx of 13 ppm at TIT of 1329 K when using diesel fuel [23]. Other simulations investigated MGT life cycle analysis, greenhouse effect and combustion characteristics of natural gas blends with ammonia and methanol [24].

Fuel spray characteristics is essential for liquid biofuels combustion. For reciprocating internal combustion engines, ignition delay when using higher viscosity fuels such as biodiesel compared to fossil diesel presents a major issue [25]. However, this issue is not of a concern in gas turbines due to the fundamentally different nature of combustion utilizing steady-state combustion rather than intermittent combustion. Despite that, the poor fuel atomization and evaporation when using viscous liquid biofuels still presents a major issue since fuels with poor evaporation would require significant extension of the flame which requires modifications in combustion chamber geometry. Therefore, studying the fuel evaporation mechanism and how to enhance it is a priority to utilize low-grade liquid biofuels in gas turbines. A droplet evaporation model of biodiesel fuels which is based on theory continuous mixture was investigated. The model was compared to single suspended droplets experiments and was in good agreement with the measurements within 3% error [26]. The evaporation spray and combustion features of wide range of ethanol–gasoline blends (E0-E100) were investigated using a constant volume vessel with single-hole-type nozzle. The result reveals that the ethanol evaporates more than gasoline. According to difference in boiling points, a vapor ambient-gas recognizable layer mixture is constructed in the E85 spray [27].

The viscosity of vegetable oil of 80.7 mm^2/s is about one order of magnitude higher than diesel (3.6 mm^2/s) whereas biodiesel is only slightly higher than diesel (5.9 mm^2/s) [28]. The use of fuel pre-heaters to reduce the viscosity of biofuels is one of the oldest utilized methods. However, using exhaust hot gas or other preheat methods can cause fuel fouling and blockage due to fuel coking at the hot surfaces, additional to the creation of gas pockets inside fuel lines that can cause pressure fluctuation [29]. MGT performance was tested with diesel as the benchmark fuel compared to externally pre-heated biodiesel and vegetable oil using electrical heaters [28]. A method of diesel evaporation without the use of atomization injectors was tested. Superheated steam thermal power from steam injector is used to evaporate liquid diesel in a container at the bottom of the burner which can be suitable for high viscosity fuels [30]. However, this was tested with atmospheric burner, and the stability for such a design in gas turbine applications is questionable. The changes of spray patterns and vaporization behaviour for flash-boiling multi-hole sprays over a wide range of superheated conditions were studied using Mie-scattering and Laser-induced-exciplex- fluorescence (LIEF) optical techniques. The vaporization operation was tested by using the LIEF optical technique for n-hexane, providing the relative vapor quantity throughout the spray transformation process. The correlations of the spray structural change and extent of vaporization with increasing superheated

degree provided good insight into the mechanisms responsible for the observed behaviours during flash-boiling conditions [30]. Using vibration analysis [31] and combustion acoustic analysis [32] to analyse the effect of poor atomization of biofuels on combustion stability was also investigated. The Dielectric-Barrier-Discharge (DBD) plasma actuator was experimentally used to measure it is ability in micro combustors on the air flow based controlling. Smoke generator was used in experiments. The results shows that the generated plasma has small effects of the characteristics of flow while the temperature of plasma has a maximum of 90˚C when it is generated continuously [33]. Neon-oxygen was investigated for the hydrogen ignition stabilization with the ambient intake condition standard using CFD modelling. The results showed that the mean value of the initial hydrogen temperature in the neon-oxygen atmosphere was lower as compared to oxygen-argon [34]. CFD modelling has proven to be a useful tool for the optimization of turbine geometry and flow characteristics to increase the power coefficient of the turbine in effective way before testing the geometry experimentally [35].

In this paper, an evaporation process of palm oil fuel was studied numerically using CFD simulation with DPM model to imitate fuel atomization and evaporation. A novel pre-evaporation chamber geometry was investigated utilizing exhaust gas recirculation and strong swirling motion for the evaporation of the fuel.

2. Methodology

For the design of the pre-evaporation chamber, SolidWorks (2019) and ANSYS-FLUENT software (2019) were used for the CFD numerical analysis. As for the fuel source material, palm oil is produced in abundance in Malaysia with high waste potential that can cause environmental concerns.

2.1 Fuel

Palm oil (Elaeis guianensis) was originated in Africa. It spreads in Malaysia due to the humid and wet environment [36,37]. Malaysian palm oil production has increased vastly over the last 25 years, from 2.57 million metric tons in year 1980 to 14.96 million metric tons in year 2005, due to preference for palm oil as compared to rubber and other crops [37]. Two methods are used to convert palm oil into biofuel: (1) of palm oil into methyl or ethyl esters (biodiesel) by reaction with alcohol, (2) catalytic cracking of palm oil to lower molecular hydrocarbon products [38, 39]. The fuel used in the simulation is the crude palm oil extracted from oil palm mills in Malaysia. Thermal properties of fuel which have been used to perform chamber simulation are listed in Table 1.

Table 1
Thermal properties of oil palm fuel at 30 °C [40]

Properties	Value
Density (kg/m^3)	885
Specific heat(J/Kg.°C)	1875
Viscosity (Pa.S)	0.05785
Vaporization temperature (°C)	450
Boiling Point (°C)	510

2.2 Chamber Drawing

The drawing of pre-evaporation chamber geometry prior to mesh creation is done using SolidWorks software (2019) due to its flexibility in modifying the geometry to accommodate wider range of geometry variation for the design optimization. Part of the hot exhaust gas from MGT combustion chamber is recycled into the pre-evaporation chamber where it is introduced through two tangential inlet ports to create a cyclonic motion through the chamber. A revolve chamber geometry was chosen with the revolve curvature diameter (Dr) which is circuit diameter that revolves 360° around the pre-chamber axis to create the revolve. Dr was increased from 40mm up to 90mm for the geometry optimization process. The distance between this circuit centre and the pre-chamber axis was fixed at 25mm for all designs, thus, this will give an outer diameter (Do) range of 90-140mm for the pre-chamber with 10mm increments. The number of the revolves was varied from 5 to 8 as the second manipulated variable for the geometry optimization process. The last revolve before the exit had the same Dr as the other revolves but the distance to the axis was reduced to 12.5mm resulting in an outer diameter range of 65-115mm. This reduction was designed for smooth transition to the outlet nozzle before the fuel vapour in injected to the main combustion chamber. The length of a single revolve is same as Dr and the length of the exit nozzle is 25mm. Fuel injection ports were not added physically to the chamber geometry since the use of DPM allows the alteration of injection location and the number of injectors inside the CFD settings. The general geometry of the pre-evaporation chamber is shown in Figure 1.

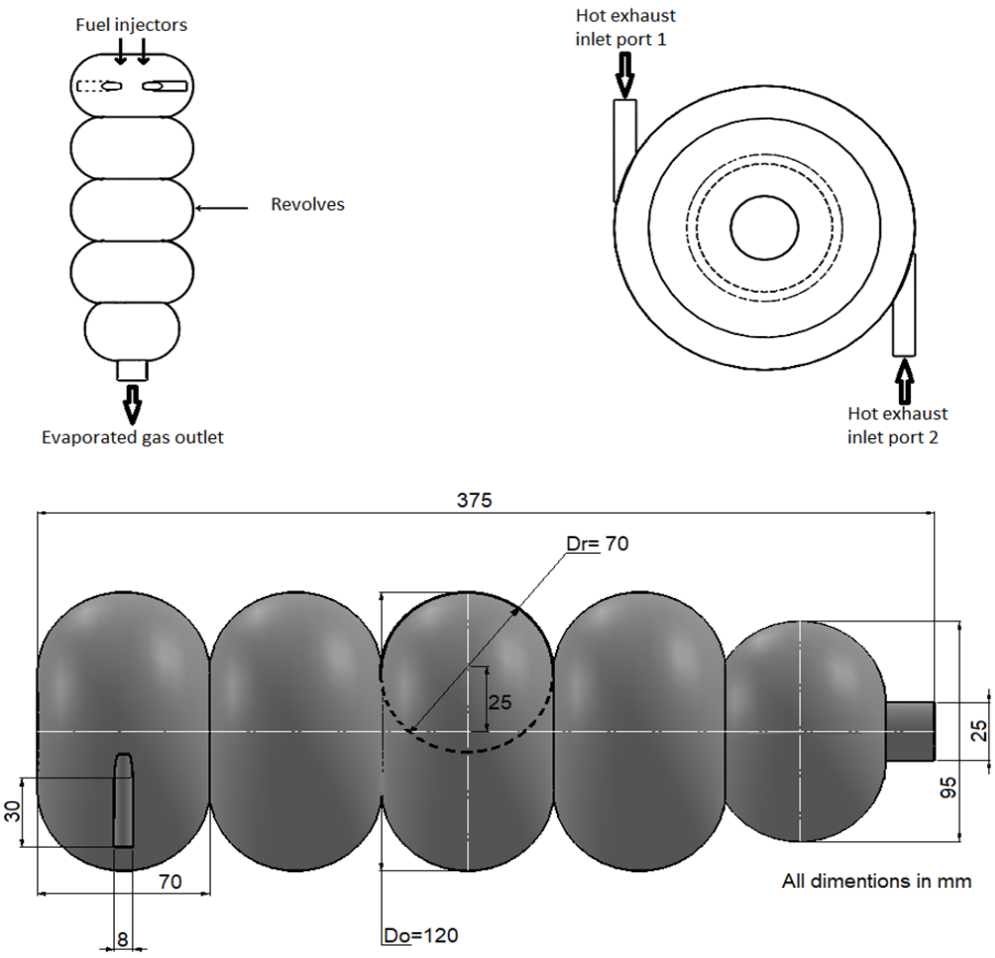

Fig. 1. Schematic of the revolve pre-evaporation chamber with 3D SOLIDWORS drawing of 5 revolves and revolve diameter of 70mm

2.3 CFD Simulation

ANSYS-Fluent software is used in order to analyzed the flow of recycle hot gas and simulate the flow of fuel inside chamber through the k-epsilon model. DPM is utilized to simulate the fuel injection and evaporation process while non-premixed model is used to identify the species of recycled hot exhaust gas.

2.3.1 Non-premixed Model Setup

In the non-premixed model, a PDF was generated in order to identify the composition of the hot exhaust recycled gas species (located under oxidizer section) as well as the palm oil fuel. It should be noticed that the PDF only specifies the properties of the species and their changes with temperature only in the gaseous form. Therefore, palm oil is identified in this model as oil vapor and not as a liquid fuel. And since the fuel (i.e., liquid palm oil) will be introduced through the fuel injectors only, thus, no boundary condition is allocated as "fuel inlet", and the only inlet boundary is for the recycled hot exhaust gas. One more thing to notice is that the original purpose of this model in ANSYS-Fluent is to simulate combustion. However, in the current study, the operating conditions of low oxygen content and temperature ensure that combustion process does not start in the pre-evaporation chamber and it is postponed to the main chamber where fuel vapor is mixed with air in the main combustion chamber. The target of CO emissions exiting the MGT combustion chamber was set to be below 100 ppm, thus, the exhaust gas from the chamber was calculated based on the chemical reaction of palm oil shown in Eq. (1). Elemental analysis of palm cooking oil available commercially in the Malaysian market revealed the mass content of the elements to be 83% carbon, 11.4% hydrogen, 2.5% nitrogen and 3% oxygen.

$$\frac{83}{12}C + \frac{11.43}{1}H + \frac{3}{16}O + \frac{2.47}{14}N + 25.62(O_2 + 3.76N_2) \rightarrow 5.69CO_2 + 1.23CO + 5.71H_2O + 16.55O_2 + 96.67N_2 \quad (1)$$

The full molar fraction for the exhaust recycled gas was then calculated from Eq. (1) and the PDF setting as molar fraction for the fuel and oxidizer (i.e., exhaust recycled gas) was then keyed in to the CFD simulation as shown in Table 2.

Table 2
Species mole fraction for PDF setup

Species	Fuel setup	Oxidizer setup
N_2	0	0.765.5
O_2	0	0.132
CO	0	0.0098
CO_2	0	0.0452
Palm oil vapor	1	0
H_2O	0	0.0454

2.3.2 DPM and Viscosity Models Setup

The k-ε model was used in this study since it suitable for flow with swirling motion. Heat transfer and turbulence behavior can be predicted through standard k-ε model. This model is based on two transport equations for the turbulence kinetic energy (k) and its dissipation rate (ε) shown as Eq. (2) and Eq. (3).

$$\frac{\partial}{\partial \mathrm{t}}(\rho k)+\frac{\partial}{\partial x_i}(\rho k u_i)=\frac{\partial}{\partial x_j}\left[\left(u+\frac{u_t}{\sigma_k}\right)\frac{\partial k}{\partial x_j}\right]+G_k+G_b-\rho\varepsilon-Y_M+S_k \quad (2)$$

$$\frac{\partial}{\partial \mathrm{t}}(\rho \varepsilon)+\frac{\partial}{\partial x_i}(\rho \varepsilon u_i)=\frac{\partial}{\partial x_j}\left[\left(u+\frac{u_t}{\sigma_\varepsilon}\right)\frac{\partial \varepsilon}{\partial x_j}\right]+C_{1\varepsilon}\frac{\varepsilon}{k}(G_k+C_{3\varepsilon}G_b)-C_{2\varepsilon}\rho\frac{\varepsilon^2}{k}+S_\varepsilon \quad (3)$$

where, Gk and Gb are turbulence kinetic energy generation by mean velocity and buoyancy; YM is fluctuating dilatation contribution in compressible turbulence to the overall dissipation rate; C_1ε,C_2ε,C_3ε are constants; ρk,ρε are turbulent Prandtl numbers for k, ε. The heat losses through the outer walls was set as a fixed heat flux of 12.9 kW/m2 calculated from the expected efficiency of this chamber. Discreet phase model used to imitate the injection of fuel particles with 1 to 3 injectors tests. For the single injector setup, the injector is located at the centre axis of the chamber while two and three injector setups are arranged radially with 180° and 120° angle, respectively, between the injectors. Chamber axis is on X-axis, and the injection stream velocity for the Y & Z axes was changed from 0.6 m/s in the axis direction then drops to zero for the central stream then increases to 0.6 m/s in the opposite direction. Therefore, only the central injection stream travels parallel to the chamber axis while the two streams (on each side) are pushed tangentially towards Y & Z axes creating a swirl injector motion with 30° injector angle to match the specification of the commercially available fuel injectors that will be used in the experimental phase of this project. The boundary conditions of the pre-evaporation chamber and DPM injector setup for three injector mode with multiple droplets is shown in Table 3. The gas inlet condition is set to mass flow inlet, with normal-to-boundary setup, while outlet is set to pressure outlet. There is no fuel inlet boundary condition since the fuel injection is handled by the DPM.

Table 3
Boundary conditions and DPM 3-injector setup

Parameters	Values	Parameters	Values
Fuel input (DPM)		Gas inlet (mass flow inlet)	
Particle type	Droplet	Temperature (K)	1223
Injection type	Group	Pressure	1atm
Number of streams	5	Mass flowrate (kg/s)	0.0042365
Mass flowrate (kg/s)	0.000174	Turbulent viscosity intensity	5%
X-velocity (m/s)	+1	Turbulent viscosity ratio	10
Y-velocity	+0.6 to -0.6		
Z-velocity (m/s)	+0.6 to -0.6	Walls	
Temperature (K)	300	Heat Flux (W/m^2)	12946
		Thickness (mm)	3
Outlet (pressure outlet)		DPM	reflect
Pressure	1atm		
Back flow temperature (K)	1000		

Two inlet ports with (8 mm diameter and 30 mm length) are attached tangentially to the pre-chamber to introduce the recycled hot exhaust gas which will be pushed in cyclonic motion inside the chamber in order to create turbulence motion inside the chamber and enhance fuel evaporation process. The gas temperature was set to 950°C throughout the simulation since turbine inlet temperature is expected to be limited. However, additional evaluation of the temperature effect on evaporation was performed on the optimum chamber geometry where gas temperature was elevated up to 1050°C. The gas recycling was fixed at 10% of the total exhaust flow rate, thus, gas flow rate to the pre-evaporation chamber was set to 0.00847 kg/s.

3. Mesh Independence Study

Figure 2 shows the mesh independence test results when varying the number of elements from 50,000 all the way up to 3,441,543 elements for the largest dimeter and number of revolves. The main respond variable is the accumulated mass flow rate of the evaporated palm oil liquid mass input. In general, the difference in DPM mass flow rate was not significant, and results became near constant with the subsequent elevation in the number of elements above 10^6 elements. It was found that any elevation in mesh size of 2,523,353 elements will result in less than 0.01% change DPM values, thus, this mesh setting was used for the simulation.

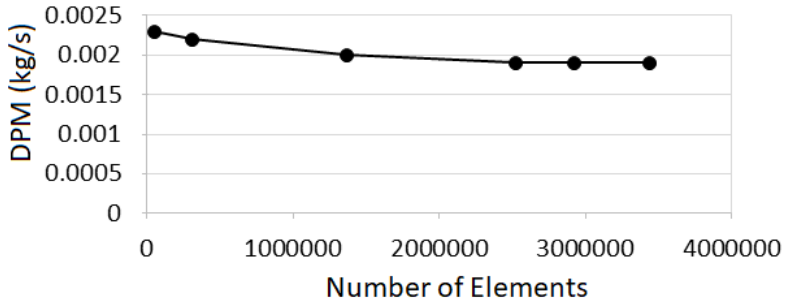

Fig.2. Mesh independence study

4. Results and Discussions

The effect of geometry changes in the form of the number of revolves, diameter of the chamber and the configuration of the injectors on the pre-evaporation chamber are discussed in this section.

4.1. Effect of Chamber Geometry

The pre-chamber performance as the number of revolves is increased from 5 to 8 and the diameter is increased from 40 to 90 mm is evaluated in this section. The general target is to achieve acceptable pre-chamber performance with minimal size that represents the least number of revolves with smallest possible diameter. The main performance indicating variable is the fuel evaporation capacity prior to the main chamber as the target is to introduce the fuel to the MGT combustion chamber mostly as vapor so it can be efficiently mixed with air which can reduce pollutant emissions considerably compared to conventional liquid-fueled MGTs. DPM was used to simulate both fuel injection and evaporation processes. The fuel inlet flow rate is 0.0026 kg/s, thus, the accumulated total mass flow rate of the evaporated fuel through the mass balance reported by DPM is compared to the fuel input to determine the fuel evaporation capacity as a percentage of the fuel input. Figure 3 shows the effect of the number of revolves and the chamber diameter on the evaporated fuel flow along with the corresponding evaporation %. Testing the two geometry variables, it was shown that minimum number of revolves to start evaporation is 5. However, having a small diameter of 40mm was not adequate to pre-evaporate the fuel with 0.00057 kg/s evaporated fuel which corresponded to only 22% fuel evaporation. This low number of revolves required the increment of chamber diameter which enhanced the evaporation gradually reaching nearly 87% evaporation at maximum diameter of 90mm. On the other hand, geometries with 7 and 8 revolves showed different performance trend where the evaporation peaked at 88.5% when reaching 70mm and 80 mm diameters, but then dropped at 90mm diameter.

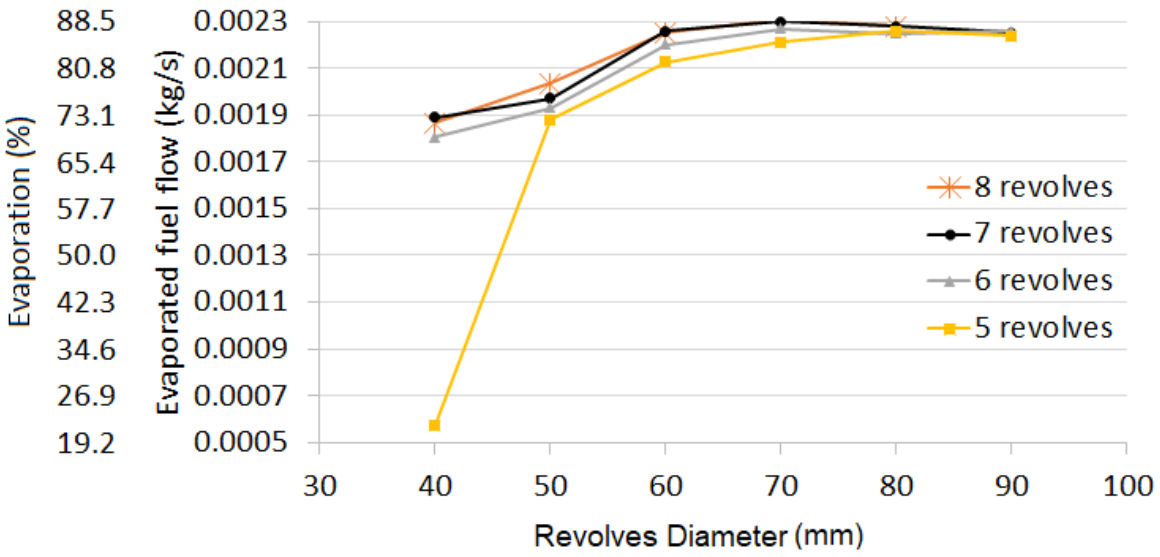

Fig. 3. Effect of number of revolves and diameter on fuel evaporation

Figure 4 show the effect of diameter and number of revolves on tangential velocity at the exit. Observing the tangential velocity profiles at the pre-chamber exit showed similar trend where 70mm and 80mm diameter at 7 and 8 revolves geometries showed low values indicating that the swirling motion was totally converted to axial motion at the exit. All other lower and higher diameters but still sharing similar chamber length (i.e., number of revolves) showed higher swirling motion at the chamber exit which was associated with lower fuel evaporation. The velocity was affected by the change of diameter since flow rate was kept as constant. Therefore, at small diameters, strong swirling motion extended all the way to the chamber exit pushing fuel droplets to the walls by the centrifugal force which reduce the interaction between the hot gas and droplets resulting in less evaporation. As for the effect of number of revolves, increasing the number has shown a considerable reduction in swirling motion as evident by the reduction of tangential velocity at the exit. Two factors are expected to affect the flow hydrodynamics when passing through the revolves along the chamber. First factor is the flow friction that increases with the number of revolves, but this factor is less pronounced at large diameters as friction losses become negligible. Second factor is the compression and de-compression effects at the inlet and exit of each revolve as this geometry does not resemble a simple cyclonic or screw chamber. At very large diameters such as 90mm, the effect of compression and de-compression become less pronounced as the flow rate is not enough to carry the effect at such large diameter. Therefore, 70mm and 80mm diameter presented an optimal size for this specific flow rate for this chamber. In conclusion, swirling motion is needed at the earlier stages where the fuel mist is concentrated and needs to be vigorously mixed with the hot gas to enhance heat transfer from the gas to the fuel. The other major mechanism to aid evaporation is the periodic compression and de-compression of flow that disturbs the swirling motion downstream the chamber that should be maintained by maintaining the balance between the flow and the diameter of the revolves.

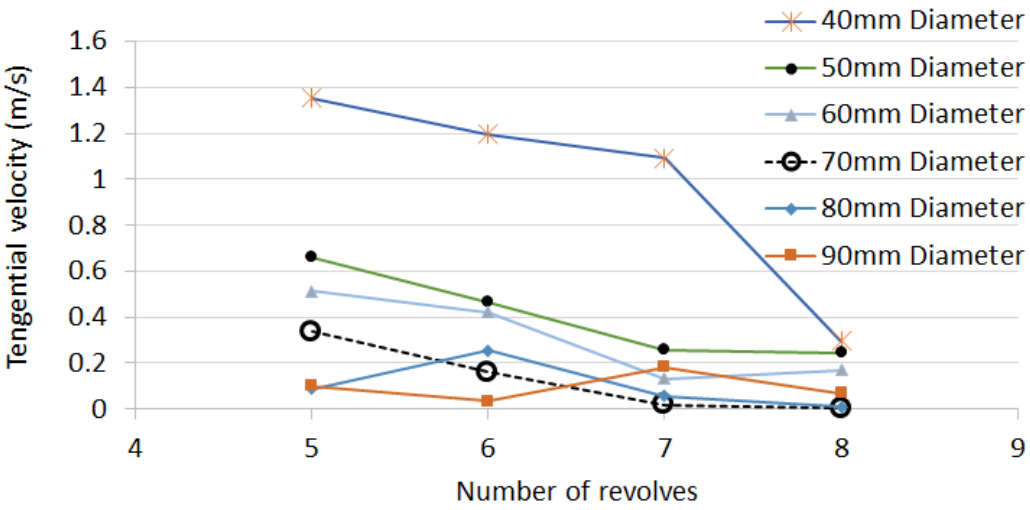

Fig. 4. Effect of geometry variables on outlet tangential velocity

Mean mixture fraction (MMF) is another important performance indicating variable. MMF is used to indicate the molar fraction in PDF (as vapor form) where MMF = 1 for fuel inlet and MMF = 0 for the oxidizer inlet. Therefore, both the dilution of fuel by the oxidizer stream (i.e., recycle exhaust gas) as well as the evaporation of fuel are indicated by MMF values. Figure 5 shows the effect of increasing the number of revolves and chamber diameter on MMF values. The findings are similar to those of the DPM flow of the evaporated fuel showing the worst case to be with 5 revolves and 40mm diameter where molar fraction of fuel vapor was only 6% of the total flow exiting the pre-chamber. On the other hand, MMF was less sensitive to the changes in geometry and did not reveal the minute effects of geometry due to the high gas dilution. Therefore, MMF can still be used as a general indicator of the performance to show roughly the acceptable geometry limits. MMF showed that geometries with diameters above 60mm and 6 revolves produces vapor fuel molar fraction of about 21% at the pre-chamber exit. It should be noticed that, as MGTs normally operate at much higher excess air supply compared to other technologies such as boilers and IC engines, the recycling of exhaust gas will provide considerable amount of oxygen. Thus, making the gas stream exiting the pre-evaporation chamber as partially mixed fuel stream, which can shorten flame extent inside the combustion chamber as the length of premixing zone will be shorter. In the current design with 10% exhaust recycling flow and 21% fuel mole fraction, oxygen molar fraction in the premixed fuel stream will be 10.4% which is still slightly beyond the rich flammability limit of the fuel. Therefore, preignition will not occur in the pre-evaporation chamber.

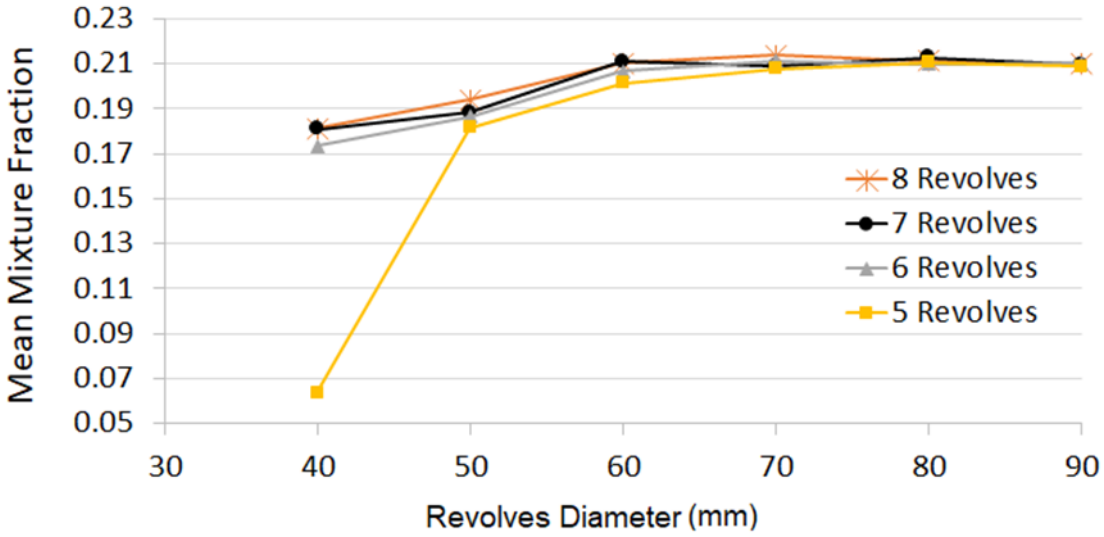

Fig. 5. Effect of number of revolves and diameter on mean mixture fraction

Results showed the minimum geometry that can achieve best evaporation was at 70mm diameter and 7 revolves. Two major factors that influence the evaporation process are the temperature and velocity magnitude. Therefore, the contours of overall temperature and velocity magnitude along the pre-chamber were investigated as shown in Figure 6. As the oxygen content at the hot exhaust recycled gas tangential inlet is about 10.4%, spontaneous ignition occurs near the wall leading to a sudden spike in temperature (around 1900K). However, the flame extinguishes immediately when pushed toward the centre due to the high fuel concentration. The temperature drops drastically to 1430K and then it gradually decreases along the pre-chamber length due to the heat losses through the outer walls. Despite the drop in temperature, the average outlet temperature was around 1330K (1057°C) which is still way above the fuel vaporization temperature of 450°C. The velocity contour demonstrated the flow hydrodynamics where the flow started tangentially with high velocity (around 20m/s) which generated the centrifugal effect where the mass was pushed to the walls creating low pressure and slow flow at the centre. The second effect of flow compression then de-compression when passing through the revolves can also be seen from the velocity profile. At the third revolve, the sudden expansion created a low pressure (and low flow velocity) zone at the centre which collapsed when the revolve started to converge again, creating the compression effect. However, this effect gradually faded towards the exit as the velocity dropped significantly near the walls due to friction and the tangential flow started to convert into axial flow. The last change in the velocity is at the outlet nozzle where the flow is compressed again as a preparation for the fuel injection into the main chamber.

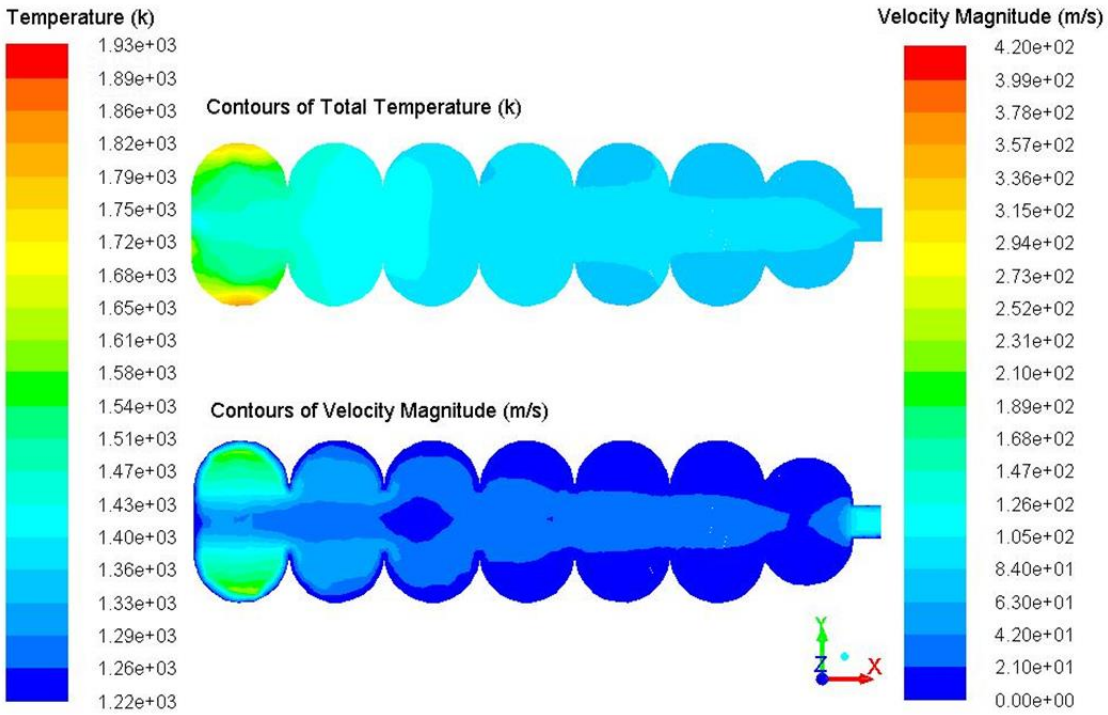

Fig. 6. Temperature and velocity distribution contours for the optimum geometry

Using vehicular turbocharger as the base for the MGT development will limit turbine inlet temperature below 1000°C to avoid damaging turbine blades. Therefore, 950°C recycled exhaust gas temperature was chosen for the chamber optimization process. However, further investigation was made to test the effect of higher temperatures (1000 & 1050°C) on the evaporation process as shown in Figure 7. As expected, increasing gas temperature enhanced the evaporation of the fuel as the evaporation process is mainly dependent on the thermal power transferred from the surrounding gasses to the fuel droplet to provide the needed latent heat of evaporation. However, it was noticed that the enhancement of evaporation was not significant resulting in less than 1% increment in evaporation at the highest temperature of 1050°C compared to the optimum case. Therefore, elevating the recycled gas temperature above 950°C is not recommended as it will increase the piping insulation and maintenance requirement without considerable enhancement of the pre-evaporation chamber performance.

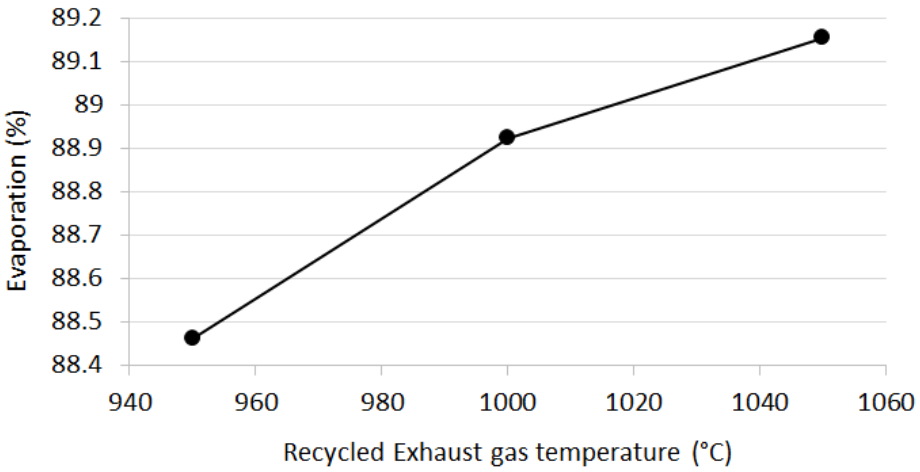

Fig. 7. Effect of hot gas inlet temperature on fuel evaporation using the optimum geometry

4.2 Effect of Number of Injectors

For the MGT setup, having a single fuel injector is the most economical option in terms of the initial cost as well as the maintenance cost and requirement. However, when using single injector, large injector nozzle is needed to accommodate the large flow rate as all the fuel will be passed through this single injector. As expected, single injector provided the lowest evaporation as the exposed surface area of the fuel to perform the evaporation process is minimal as the fuel streams were limited to 5 per injector resulting in around 73% fuel evaporation as shown in Figure 8. On the other hand, three injectors provided 15 fuel streams and wider distribution of the fuel which provided better gas-fuel mixing and higher evaporation exceeding 88%.

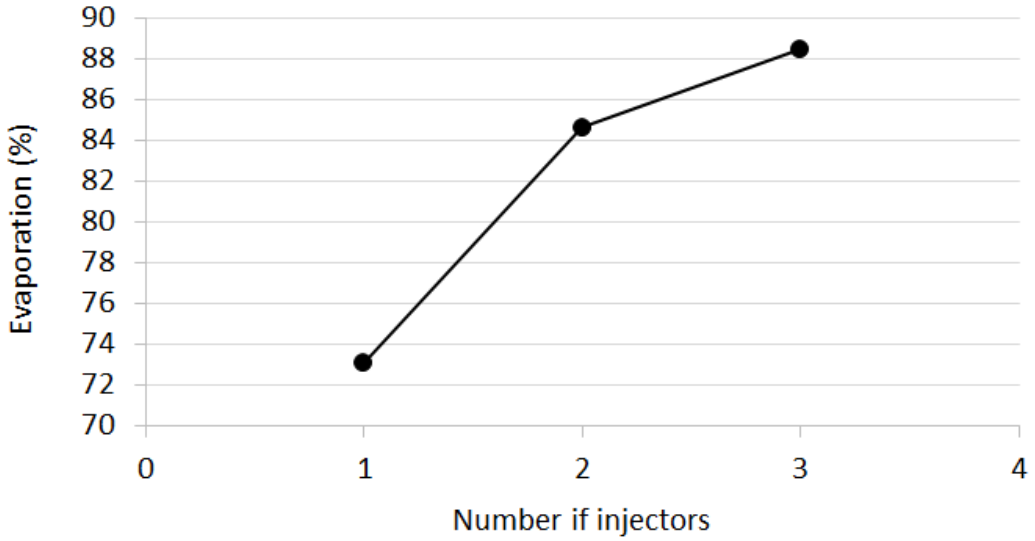

Fig. 8. Effect of number of injectors on fuel evaporation

In order to study the quality of fuel distribution across the pre-chamber, fuel particle tracking based on evaporation time was used as shown in Figure 9. Having a single injector at the center of the pre-evaporation chamber extended the axial spray penetration without being mixed with the hot exhaust gas which represented the major downside of using single injector from the hydrodynamic flow point of view. On the other hand, shifting the injectors off-center in 2 &3 injector configurations eliminated this issue, where hot gas stream contacts the fuel droplets in a cross-flow manner spreading the droplets in the first revolve to maximize heat transfer before the gases cool down along the chamber.

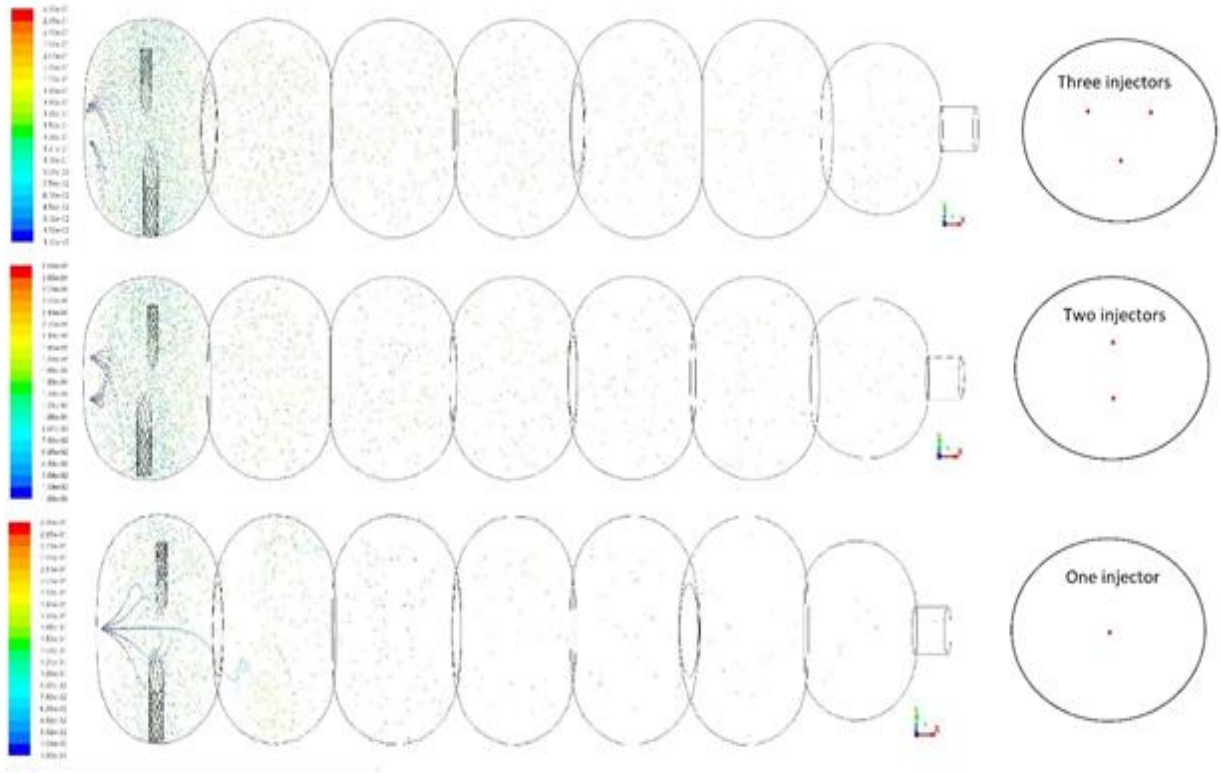

Fig. 9. Injector particle tracking based on evaporation residence time for 1, 2 and 3 injectors

5. Conclusions

In this study, a novel pre-evaporation chamber was designed. It included several revolves that provide two major mechanisms to aid the fuel evaporation. First mechanism is the swirling motion at the injectors which provide cross-flow interaction between fuel droplets with hot gas in cyclonic motion which enhances the heat transfer process. The second mechanism is the compression and de-compression effects at the inlet and the exit of each revolve that ensures continuous gas-liquid interaction and prevents the droplets from being pushed to the chamber walls by the centrifugal force. However, this second mechanism can only be maintained by maintaining the balance between the flow and the diameter of the revolves. Minimum number of revolves to start the evaporation was found to be 5, while increasing the diameter from 40mm to 90mm increased the evaporation from 22% up to 87%. As for the geometry effect on evaporation, best evaporation was achieved in the diameter range of 70-80mm, while increasing the number of revolves above 7 showed negative effect on evaporation. Therefore, the optimum pre-evaporation chamber was found to be 7 revolves with 70mm diameter. Further investigations were done on the optimum geometry to investigate the effect of recycled exhaust gas temperature, where the elevation from 950°C up to 1050°C resulted in less than 1% evaporation enhancement. Finally, the effect of number of injectors was investigated by testing one central injector, two and three injectors at 180° and 120° from each other, respectively. It was found that the enhancement in evaporation process was proportional to the number of injectors. The future work will include testing this new pre-evaporation chamber with an existing MGT combustion chamber to utilize different types of low-grade liquid biofuels.

Acknowledgement
The authors would like to thank the Ministry of Education Malaysia, Fundamental Research Grant Scheme (FRGS:203.PMEKANIK.6071426) for the financial support of this study.

References

[1] Samsudin M.S.N., Rahman M.M., and Wahid M.A. " Sustainable Power Generation Pathways in Malaysia : Development of Long-range Scenarios." *Journal of Advanced Research in Applied Mechanics,* vol. 24, no. 1 (2016): 22–38.

[2] Hudda, N., Durant, L. W., Fruin, S. A., & Durant, J. L. "Impacts of aviation emissions on near-airport residential air quality". *Environmental Science & Technology*, vol.54, no.14 (2020): 8580-8588. https://doi.org/10.1007/s11270-020-04933-z.

[3] Grobler, C., Wolfe, P. J., Dasadhikari, K., Dedoussi, I. C., Allroggen, F., Speth, R. L., ... & Barrett, S. R. "Marginal climate and air quality costs of aviation emissions". *Environmental Research Letters*, vol.14, no.11 (2019): 114031. https://doi.org/10.1088/1748-9326/ab4942

[4] Nicolini, M., & Tavoni, M. "Are renewable energy subsidies effective? Evidence from Europe". *Renewable and Sustainable Energy Reviews*, vol, 74 (2017): 412-423. https://doi.org/10.1016/j.rser.2016.12.032

[5] Yacob N.S., Mohamed H., and Shamsuddin A.H. "Investigation of Palm Oil Wastes Characteristics for Co-firing with Coal," *Journal of Advanced Research in Applied Sciences and Engineering Technology* vol. 23, no. 1 (2021): 34-42.

[6] Colak I., Sagiroglu S., Demirtas M., and Yesilbudak M. "A data mining approach: Analyzing wind speed and insolation period data in Turkey for installations of wind and solar power plants," *Energy Convers. Manag.*, vol. 65 (2013): 185–197. http://dx.doi.org/10.1016/j.enconman.2012.07.011

[7] Zhou C., Doroodchi E., and Moghtaderi B. "An in-depth assessment of hybrid solar-geothermal power generation," *Energy Convers. Manag.*, vol. 74 (2013): 88–101. http://dx.doi.org/10.1016/j.enconman.2013.05.014

[8] Hosseini S.E., Andwari A.M., Wahid M.A., and Bagheri G. "A review on green energy potentials in Iran," *Renew. Sustain. Energy Rev.*, vol. 27 (2013): 533–545, http://dx.doi.org/10.1016/j.rser.2013.07.015

[9] Demirbas A., "Waste management, waste resource facilities and waste conversion processes," *Energy Convers. Manag.*, vol. 52, no. 2 (2011): 1280–1287. http://dx.doi.org/10.1016/j.enconman.2010.09.025

[10] Corro G., Pal U., Bañuelos F., and Rosas M. "Generation of biogas from coffee-pulp and cow-dung co-digestion: Infrared studies of postcombustion emissions," *Energy Convers. Manag.*, vol. 74 (2013): 471–481. http://dx.doi.org/10.1016/j.enconman.2013.07.017

[11] Khalil A.E.E. and Gupta A.K. "Clean combustion in gas turbine engines using Butyl Nonanoate biofuel," *Fuel*, vol. 116 (2014): 522–528. http://dx.doi.org/10.1016/j.fuel.2013.08.022

[12] Sundararaj, R.H, Kumar, R.D., Raut, A.K., Sekar, T.C., Pandey, V., Kushari, A., Puri S.K. "Combustion and emission characteristics from biojet fuel blends in a gas turbine combustor." *Energy*, Vol. 182(2019): 689-705. https://doi.org/10.1016/j.energy.2019.06.060

[13] Boomadevi, P., Paulson V., Samlal S., Varatharajan M., Sekar M., Alsehli M., Elfasakhany A., Siriporn Tola S. "Impact of microalgae biofuel on microgas turbine aviation engine: A combustion and emission study," *Fuel*, Vol. 302 (2021): 121155. https://doi.org/10.1016/j.fuel.2021.121155

[14] Ye J., P. Medwell R., Varea E., Kruse S., Dally B.B., and Pitsch H.G. "An experimental study on MILD combustion of prevaporised liquid fuels," *Appl. Energy*, vol. 151 (2015): 93–101. http://dx.doi.org/10.1016/j.apenergy.2015.04.019

[15] Mahendra Reddy V. and Kumar S. "Development of high intensity low emission combustor for achieving flameless combustion of liquid fuels," *Propuls. Power Res.*, vol. 2, no. 2 (2013): 139–147. http://dx.doi.org/10.1016/j.jppr.2013.04.006

[16] Reddy V.M., Katoch A., Roberts W.L., and Kumar S. "Experimental and numerical analysis for high intensity swirl based ultra-low emission flameless combustor operating with liquid fuels," *Proc. Combust. Inst.*, vol. 35, no. 3 (2015): 3581–3589. http://dx.doi.org/10.1016/j.proci.2014.05.070

[17] Jaat N., Khalid A., Mustaffa N., Zulkifli F.H., Sunar N.M., Nursal R.S., Mohamad M.A.M., Didane D. "Analysis of Injection Pressure and High Ambient Density of Biodiesel Spray using Computational Fluid Dynamics," *CFD letters*, vol. 11, no. 1 (2019): 28–39.

[18] Hashimoto N., Ozawa Y., Mori N., Yuri I., and Hisamatsu T. "Fundamental combustion characteristics of palm methyl ester (PME) as alternative fuel for gas turbines," *Fuel*, vol. 87 (2008): 3373–3378. http://dx.doi.org/10.1016/j.fuel.2008.06.005

[19] Kurji H., Valera-Medina A., Runyon J., Giles A., Pugh D., Marsh R., Cerone N., Zimbardi F., Valerio V. "Combustion characteristics of biodiesel saturated with pyrolysis oil for power generation in gas turbines," *Renew. Energy*, vol. 99, (2016): 443–451. http://dx.doi.org/10.1016/j.renene.2016.07.036

[20] Suchocki, T., Witanowski, L., Lampart, P., Kazimierski, P., Januszewicz, k., Gawron, B. "Experimental investigation of performance and emission characteristics of a miniature gas turbine supplied by blends of kerosene and waste tyre pyrolysis oil," *Energy*, Vol. 215, Part A (2021): 119125. https://doi.org/10.1016/j.energy.2020.119125

[21] Seljak T. and Katrašnik T., "Emission reduction through highly oxygenated viscous biofuels: Use of glycerol in a micro gas turbine," *Energy*, vol. 169 (2019): 1000–1011. http://dx.doi.org/10.1016/j.energy.2018.12.095
[22] Enagi I.I., Al-attab K.A., and Zainal Z.A. "Combustion chamber design and performance for micro gas turbine application," *Fuel Process. Technol.*, vol. 166 (2017): 258–268. http://dx.doi.org/10.1016/j.fuproc.2017.05.037
[23] Enagi I.I., Al-attab K.A., and Zainal Z.A. "Liquid fuels spray and combustion characteristics in a new micro gas turbine combustion chamber design." *Int. J. Energy Res.*, vol. 43, no. 8 (2019): 3365–3380. http://dx.doi.org/10.1002/er.4475
[24] Ayaz, S.K., Altuntas, O., Caliskan H.. "Enhanced life cycle modelling of a micro gas turbine fuelled with various fuels for sustainable electricity production," *Renew. Sustain. Energy Rev.*, Vol. 149 (2021): 111323. https://doi.org/10.1016/j.rser.2021.111323
[25] Das M., Sarkar M., Datta A., and Santra A.K. "An experimental study on the combustion, performance and emission characteristics of a diesel engine fuelled with diesel-castor oil biodiesel blends," *Renew. Energy*, vol. 119 (2018): 174–184. http://dx.doi.org/10.1016/j.renene.2017.12.014
[26] Hallett W.L.H. and Legault N.V. "Modelling biodiesel droplet evaporation using continuous thermodynamics," *Fuel*, vol. 90, no. 3 (2011): 1221–1228. http://dx.doi.org/10.1016/j.fuel.2010.11.035
[27] Chen R.and Nishida K. "Spray evaporation of ethanol-gasoline-like blend and combustion of ethanol-gasoline blend injected by hole-type nozzle for direct-injection spark ignition engines," *Fuel*, vol. 134 (2014): 263–273. http://dx.doi.org/10.1016/j.fuel.2014.05.082
[28] Chiaramonti D., Rizzo A.M., Spadi A., Prussi M., Riccio G., and Martelli F. "Exhaust emissions from liquid fuel micro gas turbine fed with diesel oil, biodiesel and vegetable oil," *Appl. Energy*, vol. 101 (2013): 349–356. http://dx.doi.org/10.1016/j.apenergy.2012.01.066
[29] Broumand, M., Khan M.S., Yun, S., Hong Z., Thomas M.J. "Feasibility of running a micro gas turbine on wood-derived fast pyrolysis bio-oils: Effect of the fuel spray formation and preparation," *Renewable Energy*, 178 (2021): 775-784. https://doi.org/10.1016/j.renene.2021.06.105
[30] Anufriev I.S., Alekseenko S.V., Sharypov O.V., and Kopyev E.P. "Diesel fuel combustion in a direct-flow evaporative burner with superheated steam supply," *Fuel*, vol. 254 (2019): 115723. http://dx.doi.org/10.1016/j.fuel.2019.115723
[31] Capasso, R., Langella, G., Niola, V., Quaremba, G. "The impact of biofuel properties on emissions and performances of a micro gas turbine using combustion vibrations detection," *Fuel Processing Technology*, Vol. 179 (2018): 10-16. https://doi.org/10.1016/j.fuproc.2018.06.003
[32] Enagi I.I, Al-attab., K.A. and Zainal Z.A. "Combustion stability analysis of liquid biofuels using acoustic signals," *Journal of Advanced Research in Fluid Mechanics and Thermal Sciences*, Vol. 76 (2020): 145-155. https://doi.org/10.37934/arfmts.76.1.145155
[33] Ridzuan Tan N.D.M., Munir F. A., Tahir M.M., Saputro H. Mikami M. "Preliminary Investigation of Using DBD Plasma for Application in Micro Combustors," *Journal of Advanced Research in Micro and Nano Engineering,* vol. 1, no. 1 (2020): 50–57.
[34] Taib N.M., Mansor M.R.A., and Wan Mahmood W.M.F. "Simulation of Hydrogen Fuel Combustion in Neon-oxygen Circulated Compression Ignition Engine," *Journal of Advanced Research in Numerical Heat Transfer,* vol. 3, no. 1 (2020): 25–36. https://doi.org/10.37934/cfdl.12.12.116
[35] Sewucipto S. and Yuwono T. "The Influence of Upstream Installation of D-53 ° Type Cylinder on the Performance of Savonius Turbine," *Journal of Advanced Research in Experimental Fluid Mechanics and Heat Transfer,* vol. 3, no. 1 (2021): 36–47.
[36] Zeng W., Xu M., Zhang G., Zhang Y. and Cleary D.J. "Atomization and vaporization for flash-boiling multi-hole sprays with alcohol fuels," *Fuel*, vol. 95 (2012): 287–297 http://dx.doi.org/10.1016/j.fuel.2011.08.048
[37] Basiron Y., "Palm oil production through sustainable plantations," *Eur. J. Lipid Sci. Technol.*, vol. 109, no. 4 (2007): 289–295. http://dx.doi.org/10.1002/ejlt.200600223
[38] Chew T.L. and Bhatia S. "Catalytic processes towards the production of biofuels in a palm oil and oil palm biomass-based biorefinery," *Bioresour. Technol.*, vol. 99, no. 17 (2008): 7911–7922. http://dx.doi.org/10.1016/j.biortech.2008.03.009
[39] Agarwal A.K. and Das L.M. "Biodiesel Development and Characterization for Use as a Fuel in Compression Ignition Engines," *J. Eng. Gas Turbines Power*, vol. 123, no.2 (2001): 440–447. http://dx.doi.org/10.1115/1.1364522
[40] CHEMPRO-2021. Chempro-Edible- Oil Refining. http://chempro.in/palmoilproperties.htm [Accessed in March 2021].